



This is a repository copy of *Fabrication of Self-Cleaning, Reusable Titania Templates for Nanometer and Micrometer Scale Protein Patterning*.

White Rose Research Online URL for this paper:
<http://eprints.whiterose.ac.uk/86921/>

Version: Accepted Version

Article:

Moxey, M., Johnson, A., El-Zubir, O. et al. (6 more authors) (2015) Fabrication of Self-Cleaning, Reusable Titania Templates for Nanometer and Micrometer Scale Protein Patterning. ACS Nano. ISSN 1936-086X

<https://doi.org/10.1021/acsnano.5b01636>

Reuse

Unless indicated otherwise, fulltext items are protected by copyright with all rights reserved. The copyright exception in section 29 of the Copyright, Designs and Patents Act 1988 allows the making of a single copy solely for the purpose of non-commercial research or private study within the limits of fair dealing. The publisher or other rights-holder may allow further reproduction and re-use of this version - refer to the White Rose Research Online record for this item. Where records identify the publisher as the copyright holder, users can verify any specific terms of use on the publisher's website.

Takedown

If you consider content in White Rose Research Online to be in breach of UK law, please notify us by emailing eprints@whiterose.ac.uk including the URL of the record and the reason for the withdrawal request.



eprints@whiterose.ac.uk
<https://eprints.whiterose.ac.uk/>

This document is confidential and is proprietary to the American Chemical Society and its authors. Do not copy or disclose without written permission. If you have received this item in error, notify the sender and delete all copies.

Fabrication of Self-Cleaning, Reusable Titania Templates for Nanometer and Micrometer Scale Protein Patterning

Journal:	<i>ACS Nano</i>
Manuscript ID:	nn-2015-016369.R2
Manuscript Type:	Article
Date Submitted by the Author:	n/a
Complete List of Authors:	Moxey, Mark; IMRE, Johnson, Alexander; University of Sheffield, El Zubir, Osama; University of Sheffield, Department of Chemistry Cartron, Michael; University of Sheffield, Molecular Biology and Biotechnology Dinachali, Saman; IMRE, Hunter, C. Neil; The University of Sheffield, Molecular Biology and Biotechnology Saifullah, Mohammad; Institute of Materials Research and Engineering, , A*STAR (Agency for Science Technology and Research) Chong, Karen; Institute of Materials Research and Engineering, Leggett, Graham; University of Sheffield, Department of Chemistry

SCHOLARONE™
Manuscripts

1
2
3
4
5
6
7
8
9
10
11
12
13
14
15
16
17
18
19
20
21
22
23
24
25
26
27
28
29
30
31
32
33
34
35
36
37
38
39
40
41
42
43
44
45
46
47
48
49
50
51
52
53
54
55
56
57
58
59
60

Fabrication of Self-Cleaning, Reusable Titania Templates for Nanometer and Micrometer Scale Protein Patterning

Mark Moxey^{1,2} Alexander Johnson,¹ Osama El-Zubir,¹ Michael Cartron,³ Saman Safari Dinachali,² C.

Neil Hunter,³ Mohammad S. M. Saifullah,² Karen S. L. Chong,^{2} and Graham J. Leggett^{1*}*

¹Department of Chemistry, University of Sheffield, S3 7HF, United Kingdom; ²Institute of Materials Research and Engineering (IMRE), A*STAR (Agency for Science, Technology and Research), 3 Research Link, Singapore 117602, Republic of Singapore; ³Department of Molecular Biology and Biotechnology, University of Sheffield, Western Bank, Sheffield S10 2TN, United Kingdom.

*Corresponding authors. E-mail: karen-chong@imre.a-star.edu.sg, Graham.Leggett@sheffield.ac.uk.

ABSTRACT

The photocatalytic self-cleaning characteristics of titania facilitate the fabrication of re-useable templates for protein nanopatterning. Titania nanostructures were fabricated over square centimeter areas by interferometric lithography (IL) and nanoimprint lithography (NIL). Using a Lloyd's mirror two-beam interferometer, self-assembled monolayers of alkylphosphonates adsorbed on the native oxide of a Ti film were patterned by photocatalytic nanolithography. In regions exposed to a maximum in the interferogram, the monolayer was removed by photocatalytic oxidation. In regions exposed to an intensity minimum, the monolayer remained intact. After

1
2
3 exposure, the sample was etched in piranha solution to yield Ti nanostructures with widths as
4
5 small as 30 nm. NIL was performed by using a silicon stamp to imprint a spin-cast film of titanium
6
7 dioxide resin; after calcination and reactive ion etching, TiO₂ nanopillars were formed. For both
8
9 fabrication techniques, subsequent adsorption of an oligo(ethylene glycol) functionalized
10
11 trichlorosilane yielded an entirely passive, protein-resistant surface. Near-UV exposure caused
12
13 removal of this protein-resistant film from the titania regions by photocatalytic degradation,
14
15 leaving the passivating silane film intact on the silicon dioxide regions. Proteins labeled with
16
17 fluorescent dyes were adsorbed to the titanium dioxide regions, yielding nanopatterns with bright
18
19 fluorescence. Subsequent near-UV irradiation of the samples removed the protein from the
20
21 titanium dioxide nanostructures by photocatalytic degradation facilitating the adsorption of a
22
23 different protein. The process was repeated multiple times. These simple methods appear to yield
24
25 durable, re-useable samples that may be of value to laboratories that require nanostructured
26
27 biological interfaces but do not have access to the infrastructure required for nanofabrication.
28
29
30
31

32 33 34 KEYWORDS

35
36 Nanofabrication, photolithography, nanoimprint lithography, interferometric lithography, titania,
37
38 photocatalysis, protein arrays
39
40

41
42 The organization of proteins at surfaces is necessary for applications in array-based biosensor
43
44 technology,¹⁻⁴ and for fundamental work that aims to examine the relationship between the spatial
45
46 organization of biological molecules and diverse phenomena including tissue cell attachment,⁵⁻⁸
47
48 actin filament formation,⁹ neuronal guidance, membrane protein function, biological recognition
49
50 and energy transfer in light-harvesting complexes.^{10,11} There has been a great deal of interest in the
51
52 development of techniques for the organization of proteins on nanometer length scales, but to date
53
54 there have been few reports of methods that provide control over protein organization on sub-100
55
56 nm length scales. Protein patterning is highly challenging because proteins adsorb strongly and
57
58
59
60

1
2
3 irreversibly to most surfaces; rigorous control of non-specific adsorption is required
4
5 simultaneously with the definition of protein-binding regions. Examples to date include the use of
6
7 micro-contact printing,¹² colloidal self-assembly, dip-pen nanolithography,^{13,14} nanoshaving,¹⁵
8
9 electron-beam lithography^{16,17} and near-field optical techniques.¹⁸⁻²⁰ However, local probe and
10
11 electron-beam techniques are serial in nature and thus not well suited to large area fabrication.
12
13 Moreover, samples fabricated in this way are “single-use” materials that cannot be reused with a
14
15 different biological adsorbate. Recently, interferometric lithography (IL) has been used to fabricate
16
17 protein nanopatterns over macroscopic (square cm) areas by photochemical degradation of novel
18
19 protein-resistant poly(cysteine methacrylate) brushes²¹ and by degradation of protein-resistant
20
21 silanes,²² with a feature size of 30 nm reported in the latter case. Such methods are attractive
22
23 because they enable rapid, inexpensive fabrication of macroscopically extended arrays of
24
25 nanostructured biomolecules, but they are still subject to the limitation that fresh substrates must
26
27 be fabricated for each experiment.
28
29
30

31
32 The photocatalytic properties of titania are well-documented.²³⁻²⁵ Irradiation by photons with
33
34 energies larger than the band gap leads to the formation of electron-hole pairs, with the
35
36 consequence that excited oxygen species are formed, leading to the oxidative degradation of
37
38 organic matter at the surface. Photocatalytic degradation processes have been used to pattern
39
40 organic resist layers including films of siloxanes,²⁶ alkylphosphonates,²⁷⁻³¹ alkylthiolates²⁷ and
41
42 graphene.³² Gradient structures have been fabricated, by using a grayscale mask to carry out
43
44 exposure,²⁷ and combination of photocatalysis with a local probe has enabled nanofabrication to be
45
46 attempted.³³ Recently, a titania-coated AFM probe was used to write 70 nm protein structures in a
47
48 protein-resistant silane film,³⁴ by exploiting the photocatalytic properties of the oxide film to cause
49
50 localized degradation of a protein-resistant silane film, rendering it adhesive.
51
52
53
54
55
56
57
58
59
60

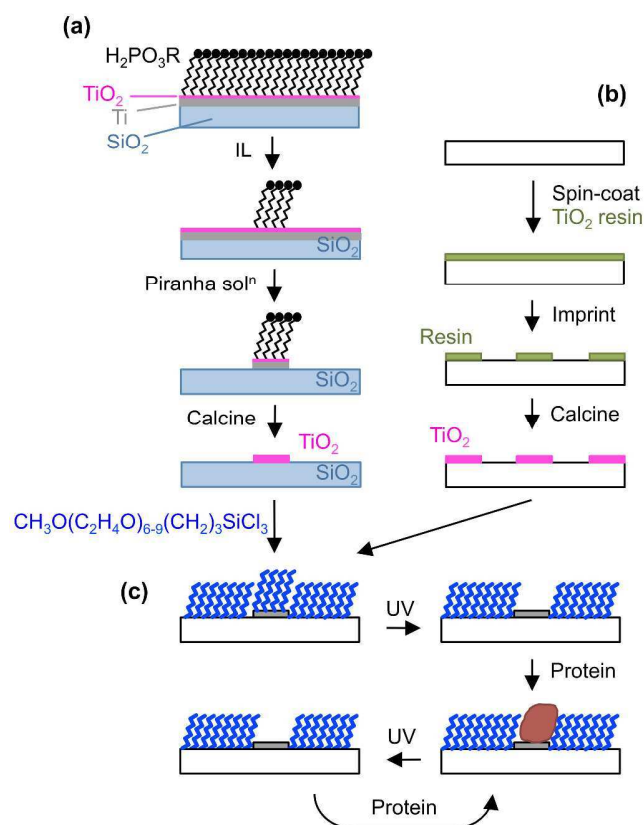


Figure 1. Schematic diagram showing the fabrication and functionalization of titanium dioxide nanostructures. (a) Photocatalytic nanopatterning of an alkylphosphonate self-assembled monolayer on titanium dioxide, by exposure to UV light in a Lloyd's mirror interferometer or through a mask, leads to selective removal of the adsorbates facilitating selective etching of the titanium dioxide film using piranha solution. (b) Nanoimprint lithography of a resin layer formed by spin-coating TiO₂ resin containing mixture of monomers onto a silicon wafer, followed by calcination, yields TiO₂ nanostructures. (c) Arrays of titania nanostructures fabricated by both approaches are coated by adsorption of an oligo(ethylene glycol) functionalized trichlorosilanes, rendering them protein-resistant. Exposure of the samples to near-UV light causes photocatalytic cleaning of titania regions, facilitating protein adsorption. Further cycles of near-UV exposure and protein adsorption may be carried out, enabling multiple re-use of samples.

1
2
3 For laboratories that are interested in the organization of proteins on nanometer length scales,
4 but do not possess extensive infrastructure for nanofabrication, the availability of re-useable
5 templates for protein adsorption, in which features are formed with high fidelity over large areas
6 (*ca.* 0.1 – 1.0 cm²), would be highly attractive. In this work we demonstrate that titania
7 nanostructures, formed by either interferometric lithography (IL)³⁵ of a self-assembled monolayer
8 (SAM) of alkylphosphonates³⁶⁻⁴² or by nanoimprint lithography (NIL) of a novel titania resin, may
9 be utilized in combination with the adsorption of protein-resistant silanes to produce nanometer-
10 scale protein patterns (Figure 1). The photocatalytic properties of the titania templates mean that
11 they may be cleaned by UV exposure, and degradation products simply rinsed away prior to re-use
12 for adsorption of a different protein.
13
14
15
16
17
18
19
20
21
22
23
24

25 RESULTS AND DISCUSSION

26 *Photolithographic Fabrication of Micro- and Nanostructures*

27
28
29
30 Micrometer- and nanometer-scale titanium structures were fabricated as shown in Figure 1(a) by
31 photocatalytic patterning of an alkylphosphonates SAM as resist. Exposure through a mask caused
32 photocatalytic degradation of the monolayer in exposed regions, while the monolayer remained
33 intact in masked regions. To create nanostructures, light from a frequency-doubled argon ion laser
34 (244 nm) was directed into a Lloyd's mirror interferometer consisting of a sample and mirror set at
35 an angle 2θ to each other; half the incident beam was directed onto the sample, and the other half
36 was reflected from the mirror onto the sample, where it interfered with the first half of the beam to
37 yield a pattern of alternating bands of constructive and destructive interference, with period
38 $\lambda/2\sin\theta$. In regions where the sample was exposed to a maximum of intensity, the adsorbates were
39 photocatalytically degraded, but in areas exposed to a minimum in the interferogram, modification
40 was limited. Consequently, when the samples were etched, using piranha solution, the titanium was
41 removed from regions exposed to a maximum in the interferogram, but in regions where the
42
43
44
45
46
47
48
49
50
51
52
53
54
55
56
57
58
59
60

sample was exposed to a band of destructive interference, the SAM remained intact and thus masked the titanium from the etch solution.

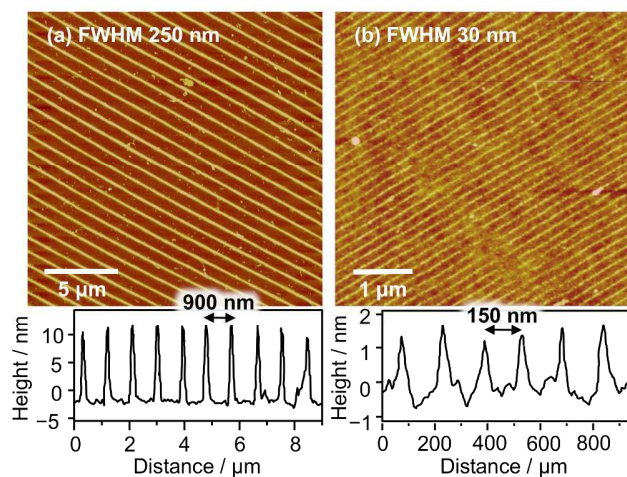


Figure 2. Tapping mode (a) and contact mode (b) AFM height images, together with representative line sections, of titanium nanowires formed by interferometric lithography. Exposure of an octadecylphosphonate SAM on the native oxide layer of a thin film of titanium was followed by etching in piranha solution.

Figure 2 shows Ti nanostructures fabricated in this fashion. The period and full width at half maximum height (FWHM) of the Ti nanostructures may be varied by changing the angle 2θ between the two interfering beams in the interferometer and by varying the etch time. In Figure 2(a), structures with a FWHM of 250 nm have been formed at a 900 nm period, while in Figure 2(b), structures with a FWHM of 30 nm have been formed at a 150 nm period. To facilitate efficient photocatalysis in subsequent protein patterning work, titanium dioxide was annealed by heating to 550 °C. It was found that annealed samples yielded higher rates of photocatalytic degradation than the as-prepared films, an observation that was attributed to the formation of the photocatalytically active anatase phase. While the titania surface used in the initial lithographic step was likely a mixture of anatase and rutile, it proved straightforward to pattern the SAMs because of the high energy of the photons (244 nm). After annealing, the titanium structures became resistant to

1
2
3 etching in piranha solution; it was thus important that calcination was carried out after the
4
5 nanofabrication process had been completed, and not beforehand.
6

7
8 TiO_2 micro- or nanostructures were immersed in a solution of
9
10 [methoxy(polyethyleneoxy)propyl]-trichlorosilane ($\text{CH}_3\text{O}(\text{C}_2\text{H}_4\text{O})_{6-9}(\text{CH}_2)_3\text{Cl}_3\text{Si}$, henceforth OEG-
11
12 silane) in toluene, to form a film of protein-resistant silane across the entire surface. Ellipsometry
13
14 indicated a thickness of *ca.* 2 nm, similar to the expected thickness of a monolayer of adsorbate,
15
16 although the thickness of the film is likely variable and ellipsometry alone cannot provide
17
18 confirmation of monolayer formation. The sample was then exposed to UV light from the HeCd laser
19
20 (325 nm), causing photocatalytic degradation of the OEG-silane molecules attached to the titania
21
22 surface and rendering those regions adhesive to proteins.
23
24

25
26 The modification of the silane film was characterized by using X-ray photoelectron spectroscopy
27
28 to characterize unpatterned films of OEG-silane formed on titanium and silicon oxide surfaces
29
30 (Figure 3). The as-prepared films on both substrates yield a strong ether component in the C1s
31
32 spectrum at 286.7 eV, together with a second component at 285.0 eV that corresponds to
33
34 hydrocarbon. After exposure of the film on titanium dioxide to a UV dose of 1.53 J cm^{-2} at 325 nm,
35
36 the ether peak was observed to be significantly reduced, and new peaks were observed at 287.8 eV
37
38 and 289.1 eV corresponding to aldehyde and carboxylic acid products of the photocatalytic
39
40 degradation process. In contrast, the C1s spectra of the films formed by adsorption of OEG-silane on
41
42 silicon dioxide surfaces showed no signs of change even after an exposure as high as 48 J cm^{-2}
43
44
45 (Figure 3(e)).
46
47
48
49
50
51
52
53
54
55
56
57
58
59
60

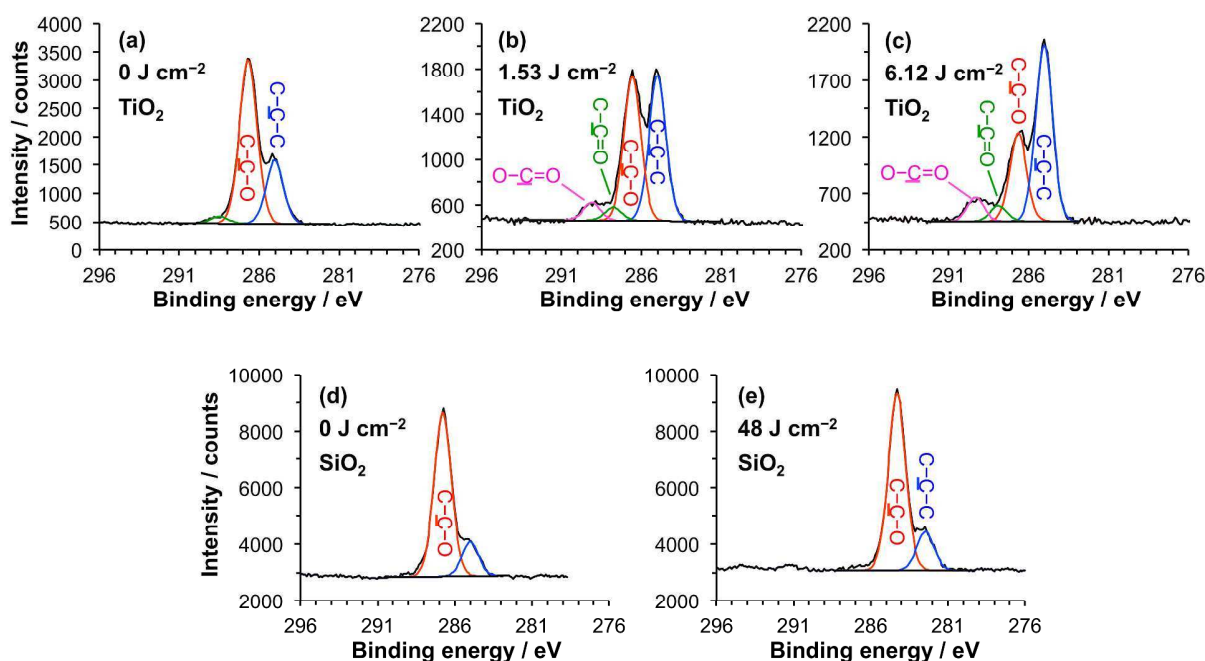
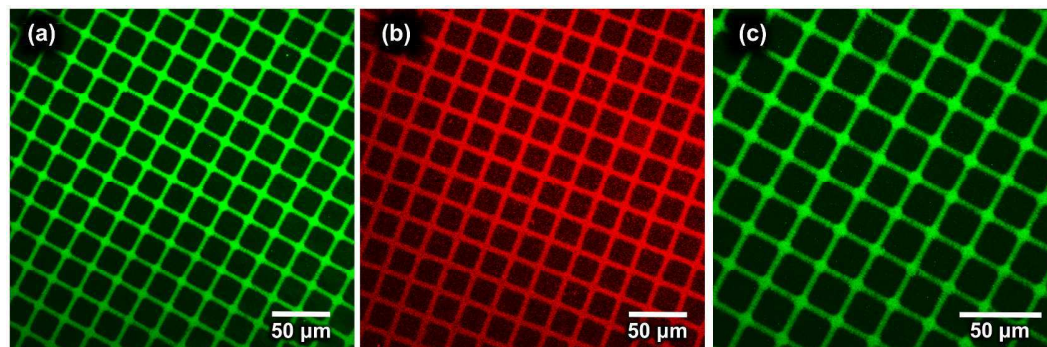


Figure 3. XPS C1s spectra for films of OEG-silane formed on titanium dioxide (a – c) and silicon dioxide (d, e) after various UV exposures at a wavelength of 325 nm.

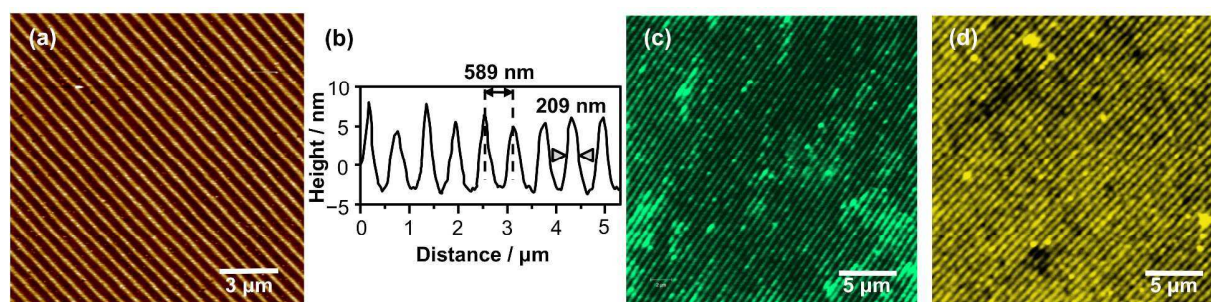
After selective removal of OEG-silane from Ti microstructures, the samples were immersed in a solution of FITC-labeled immunoglobulin G (FITC-IgG) in phosphate-buffered saline (PBS) solution. Protein adsorbed to titanium dioxide coated regions in which the surface was not protected by OEG-silane. The sample was imaged by confocal fluorescence microscopy (Figure 4 (a)). Bright green fluorescence may be observed from the TiO₂ regions (bars) but the square regions, that consist of OEG-silane-coated silicon dioxide, remain dark because the oligo(ethylene glycol) groups are highly protein resistant and remained intact in those regions.

A further exposure was carried out using the HeCd laser, to cause photocatalytic degradation of protein attached to titania. The sample was immersed in a solution of Cy3-labeled streptavidin, and imaged by confocal fluorescence microscopy (Figure 4(b)). Bright fluorescence was observed at 543 nm from the TiO₂ regions (bars) but the OEG-silane functionalized silicon dioxide regions (squares) remained dark, confirming that the streptavidin had adsorbed only to the titania surface.

1
2
3
4 Finally, the sample was cleaned by exposure at 325 nm, leading to photocatalytic breakdown of the
5 streptavidin, and the surface was refunctionalized by adsorption of FITC-IgG (Figure 4(c)).
6
7



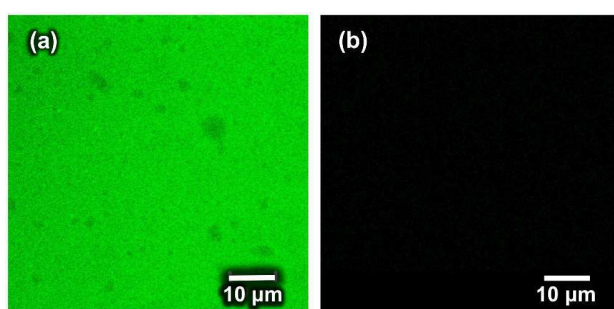
8
9
10
11
12
13
14
15
16
17
18
19
20 **Figure 4.** Confocal fluorescence microscopy images of Ti microstructures following repeated cycles
21 of photocatalytic cleaning and adsorption of (a) FITC-IgG; (b) Cy3-streptavidin; and (c) FITC-IgG.
22
23
24



25
26
27
28
29
30
31
32
33
34
35
36
37 **Figure 5.** (a) Tapping mode AFM height image of TiO₂ nanostructures fabricated for protein
38 nanopatterning experiments. (b) Line section showing a period of 589 nm and FWHM of 209 nm.
39
40 (c) Confocal fluorescence micrograph after adsorption of GFP onto the sample shown in (a). (d)
41 Fluorescence micrograph of the sample shown in (c) after photocatalytic cleaning of the TiO₂
42 nanostructures followed by adsorption of YFP.
43
44
45
46
47
48

49 Protein nanopatterns were formed on structures fabricated by interferometric lithography. To
50 enable the resulting patterns to be resolved by confocal fluorescence microscopy, a period of 589
51 nm was selected, larger than the point spread function of the imaging system. For these samples
52 (Figure 5(a)), a FWHM of 209 nm was measured. Given that some broadening of the features is
53 expected in the micrographs, these dimensions are close to the lower limit that is feasible if protein
54
55
56
57
58
59
60

1
2
3 adsorption is to be detected by fluorescence microscopy. After adsorption of green fluorescent
4 protein (GFP), clear bands of green fluorescence were observed from the TiO₂ structures (Figure
5 5(c)). The protein bands, while broadened because of the intrinsic limitations of the imaging
6 system, could clearly be resolved from the dark regions between the TiO₂ nanostructures that were
7 passivated with OEG-silane. The sample was photocatalytically cleaned, by exposure to light from
8 the HeCd laser, and immersed in a solution of yellow fluorescent protein (YFP). The YFP adsorbed
9 to the clean surfaces of the TiO₂ nanostructures, and again, the protein nanolines could be resolved
10 from the dark, OEG-passivated lines separating them (Figure 5(d)). These data demonstrate that
11 TiO₂ nanostructures may be utilized to fabricate protein nanopatterns, yielding excellent contrast in
12 fluorescence microscopy. They also demonstrate that such structures may be re-used by exploiting
13 the photocatalytic self-cleaning characteristics of titanium dioxide, with no loss of protein-
14 resistance in neighboring silicon dioxide regions that have been passivated with OEG-silane.
15
16
17
18
19
20
21
22
23
24
25
26
27
28
29



41 Figure 6. Confocal fluorescence micrographs of an unpatterned control sample before (a) and after
42 (b) photocatalytic cleaning. The mean gray scale intensity of each pixel was 64.7 AU in (a) and 2.2
43 AU in (b).
44
45
46
47

48 After exposure to the HeCd laser, both micrometer- and nanometer-scale titania patterns
49 appeared completely dark in confocal microscopy images. In an effort to quantify the removal of
50 protein in the photocatalytic step, a simple control experiment was performed using an
51 unpatterned film that had been treated in all other respects in the same way as the patterned
52 samples were. Because of the small size of the nanostructures, and the comparatively low levels of
53
54
55
56
57
58
59
60

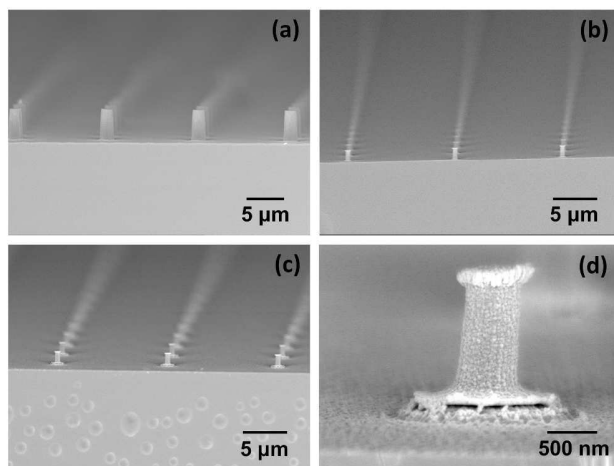
1
2
3 fluorescence detected even when they were coated with protein, a macroscopic control specimen
4
5 was judged to be a more accurate means by which to determine the efficiency of photocatalytic
6
7 cleaning. Figure 6 shows fluorescence images acquired under identical gain conditions for a
8
9 specimen before and after exposure to UV light. The mean fluorescence intensity at each pixel was
10
11 determined. Before exposure the mean intensity was 64.7 arbitrary units (AU); after exposure it
12
13 was 2.2 AU. In our microscope, the background signal is never exactly zero, and the intensity after
14
15 UV exposure, which was *ca.* 3% of the intensity beforehand, likely reflects the background noise
16
17 level in the fluorescence experiment, supporting the qualitative observation that protein
18
19 fluorescence was undetectable after photocatalytic cleaning.
20
21

22 23 *Fabrication of Protein Nanostructures by Nanoimprint Lithography*

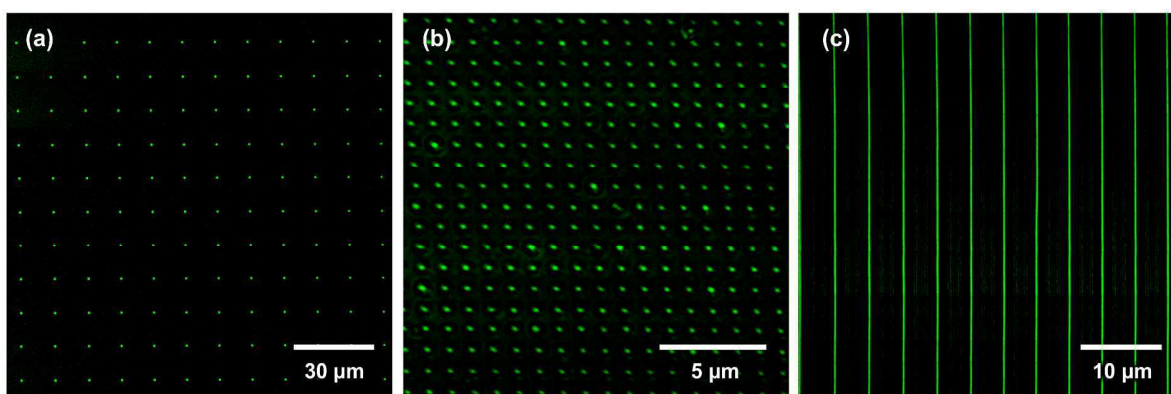
24
25 Titania nanostructures were also fabricated by nanoimprint lithography. IL and NIL are
26
27 somewhat different fabrication methods, and our goal was to determine whether titania
28
29 nanofabrication provided a generically useful approach to the fabrication of re-usable templates for
30
31 protein patterning. While NIL requires more sophisticated infrastructure than IL, it is not restricted
32
33 to the fabrication of periodic structures, as is the case for IL, offering greater freedom in the design
34
35 of nanostructures.
36
37

38
39 Titanium dioxide pillars were fabricated using NIL. The process is shown schematically in Figure
40
41 1(b). TiO₂ resin was spin-coated onto a glass substrate, and the film was patterned by NIL. Figure
42
43 7(a) shows a cross-sectional image acquired by scanning electron microscopy (SEM) for a
44
45 representative sample. The resulting structures were calcined to remove the organic components in
46
47 the imprinted film, which resulted in a 60 – 70 % shrinkage in the dimensions of the structures
48
49 (Figure 7(b)). A thin residual film remained between the nanostructures. It was difficult to resolve
50
51 by SEM, but if left intact, yielded a continuous thin film of titania between the nanostructures
52
53 defined by NIL. The residual layer was removed by reactive ion etching (RIE) in an SF₆ and Ar gas
54
55 mixture. Figure 7(c) shows the finished structures. A high magnification image of a single pillar is
56
57
58
59
60

1
2
3 shown in Figure 7(d). This micrograph shows clearly the interface between the TiO₂ pillar and the
4 SiO₂ below and surrounding it. A clear interface to the TiO₂ may be seen, confirming that it is an
5
6
7 isolated structure.
8
9

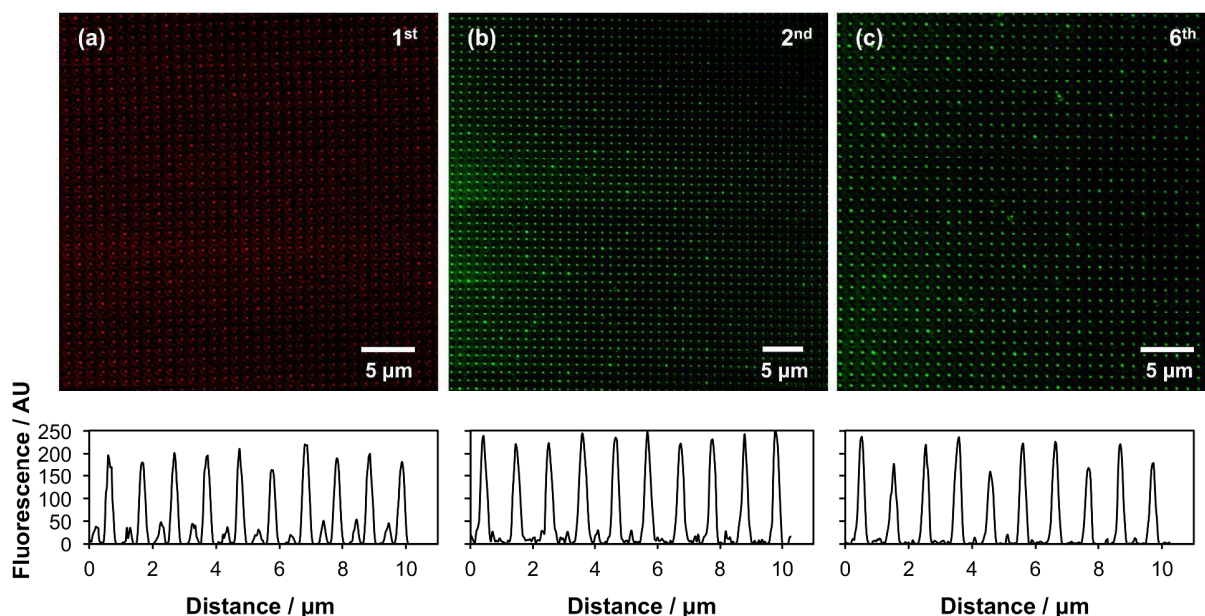


26
27 **Figure 7.** SEM cross-sectional images of (a) an array of imprinted TiO₂ resin pillars; (b) a similar
28 structure after calcination at 550 °C; (c) the finished TiO₂ structure after reactive ion etching with
29 SF₆ and Ar gasses; and (d) a high magnification image showing complete removal of the TiO₂
30
31
32 residual layer.
33
34
35



50
51 **Figure 8.** Confocal fluorescence microscopy images showing FITC-WGA adsorbed to TiO₂ patterns
52 consisting of (a) 0.6 μm dots; (b) 0.2 μm dots; and (c) 0.25 μm lines.
53
54
55
56
57
58
59
60

1
2
3 After fabrication of the array of TiO₂ pillars, OEG-silane was adsorbed onto the entire sample,
4 creating a protein-resistant layer. The sample was flooded with near-UV radiation, causing
5 photocatalytic degradation of OEG-silane molecules on the TiO₂ pillars. Protein patterns were
6 prepared by immersing the sample in a solution of fluorescein-conjugated wheat germ agglutinin
7 (FITC-WGA). Figure 8 shows confocal fluorescence microscopy images of FITC-WGA adsorbed onto
8 three different TiO₂ structures fabricated by NIL. Figures 8(a) and (b) show arrays of TiO₂ dots
9 with diameters of 600 nm and 200 nm, respectively and periods of 12 μm and 1 μm, respectively.
10 Figure 8(c) shows an array of TiO₂ lines with a width of *ca.* 250 nm and a period of 5 μm. In each
11 case, the TiO₂ nanostructures exhibit bright fluorescence, and the oxide regions between them, that
12 have been passivated using OEG-silane, exhibit dark contrast, suggesting that non-specific
13 adsorption of proteins is negligible. These data confirm the effectiveness of using TiO₂
14 nanofabrication, combined with the photocatalytic properties of the titanium dioxide surface, to
15 control protein adsorption.
16
17
18
19
20
21
22
23
24
25
26
27
28
29
30
31



54 **Figure 9.** Confocal fluorescence microscopy images of a single 0.2 μm TiO₂ dot array sample
55 following repeated cycles of protein adsorption and photocatalytic cleaning. (a) Image acquired
56
57
58
59
60

1
2
3 after the first cycle, showing Cy5-streptavidin adsorbed onto an array of TiO₂; (b) image acquired
4
5 after a second cycle, showing ITC-WGA adsorbed to titania pillars following photocatalytic cleaning
6
7 of the sample shown in (a); (c) image acquired after a sixth cycle showing FITC-WGA adsorbed to
8
9 titania pillars following consecutive adsorption and removal of FITC-WGA and Cy5-streptavidin
10
11 proteins.
12
13
14

15 Samples were subjected to repeated cycles of protein adsorption and photocatalytic cleaning.
16
17 Figure 9 shows data for a sample that consisted of 200 nm TiO₂ dots at a period of 1000 nm. The
18
19 sample was treated with OEG-silane, to render it protein-resistant, and then exposed to UV light to
20
21 remove the silane from the TiO₂ dots by photocatalytic degradation. The sample was then
22
23 immersed in a solution of Cy5-labeled streptavidin (henceforth Cy5-streptavidin) in buffer
24
25 overnight and then rinsed and imaged by confocal fluorescence microscopy (Figure 9(a)). The Cy5-
26
27 streptavidin coated TiO₂ nanodots are resolved clearly. The surrounding OEG-silane passivated
28
29 regions are dark, confirming that they remained protein-resistant. The cross-section through the
30
31 fluorescence image exhibits negligible fluorescence from these regions.
32
33
34

35 The sample was cleaned by exposure to UV light, and immersed in a solution of FITC-WGA in
36
37 buffer. The sample was rinsed and imaged by confocal fluorescence microscopy (Figure 9(b)).
38
39 Strong fluorescence is observed from the TiO₂ nanodots, and again, the cross-section through the
40
41 fluorescence micrograph shows that the fluorescence intensity from the OEG-silane regions
42
43 between the dots remains negligible.
44
45

46 The process was repeated further times. The sample was, on each occasion, cleaned by exposure
47
48 to UV light and then immersed in solutions of Cy5-streptavidin (odd numbered cycles) and FITC-
49
50 WGA (even numbered cycles). Figure 9(c) shows a fluorescence image of the sample after the sixth
51
52 cycle. Despite repeated cycles of protein adsorption and photocatalytic cleaning, the fluorescence
53
54 remains negligible on the regions between the TiO₂ nanodots, confirming that the OEG-silane is
55
56
57
58
59
60

1
2
3 resilient under near-UV exposure, and the fluorescence on the nanodots remains bright, confirming
4
5 that the protein-adhesive surface is successfully regenerated by UV exposure.
6

7 8 CONCLUSIONS

9
10 The photocatalytic self-cleaning characteristics of titania surfaces provide a simple means to
11
12 fabricate re-useable templates for protein nanopatterning. Titanium nanostructures may be
13
14 fabricated by interferometric lithography, using a simple dual-beam Lloyd's mirror interferometer
15
16 to pattern a self-assembled monolayer of alkylphosphonates on the native oxide layer of a Ti thin
17
18 film by photocatalytic degradation. The modified surface is etched with piranha solution to yield Ti
19
20 nanostructures with full widths at half maximum as small as 30 nm. Alternatively, nanoimprint
21
22 lithography may be used to pattern a spin-cast film of titanium dioxide resin that was subsequently
23
24 calcined and treated by reactive ion etching to remove residual layer from between the imprinted
25
26 structures. In both cases, the silicon oxide regions between the TiO₂ structures may be passivated
27
28 with an oligo(ethylene glycol) terminated silane, rendering them resistant to protein adsorption. In
29
30 both cases, protein can be selectively adsorbed to the TiO₂ nanostructures, and subsequently
31
32 removed by exposure to near-UV radiation, with negligible degradation of the passivating silane
33
34 film between the TiO₂ nanostructures. This facilitates multiple re-use of the TiO₂ structures as
35
36 templates for protein nanopatterning.
37
38
39

40 41 METHODS

42 43 *SAM Preparation*

44
45 Glass coverslips (Menzel-Glaser, 22 mm × 60 mm, no. 2 thickness) and silicon (100) wafers (Pi-
46
47 Kem, Tamworth, U.K.) were initially cleaned with fuming piranha solution, which is a mixture of
48
49 30% H₂O₂ and 98% concentration sulfuric acid (both purchased from Fisher scientific) in the ratio
50
51 3:7 for 40 min. (**Caution:** Piranha solution is a strong oxidizing agent, which has been known to
52
53 detonate spontaneously upon contact with organic material, and should be handled with extreme
54
55 care.) The substrates were rinsed excessively with de-ionized water and dried in an oven at 120 °C
56
57
58
59
60

1
2
3 overnight. Titanium dioxide substrates were prepared by evaporating a 15–20 nm of titanium onto
4 the glass slides at a rate of 0.03 nm s^{-1} using an Edwards Auto306 vacuum coating system. The
5 evaporator was allowed to cool before venting to dry nitrogen. To allow the formation of the native
6 oxide layer, the slides were exposed to the laboratory atmosphere for 20 min. SAMs were formed
7 on the titanium dioxide substrate by immersing them in a solution of 1 mM octadecylphosphonic
8 acid (Alfa Aesar, Heysham, UK, 97%) in toluene for 12 - 48 h. Following the formation of the SAM
9 the samples were rinsed with toluene and ethanol and dried under a stream of nitrogen.

18 *Micropatterning*

20 SAMs of ODPa on titanium were exposed in air to light from a frequency-doubled argon ion laser
21 emitting at 244 nm (Coherent FreD 300C). The laser power was measured at 33.7 mW cm^{-2} .
22 Patterns were produced by exposing the sample through a Cu TEM grid. The photo-patterned
23 samples were immersed in cold piranha solution and kept at $30 \text{ }^\circ\text{C}$ using a water bath for
24 approximately 25 min. The end point of the etching was roughly determined by eye and then later
25 confirmed by AFM, ensuring the height of the titanium features were similar to the initial
26 evaporated thickness. After etching, the samples were rinsed thoroughly with de-ionized water and
27 ethanol. The samples were calcined at $550 \text{ }^\circ\text{C}$ for 1 h.

28 SAMs of OEG-silane were formed on the etched samples by placing them in a 1 mM solution of 2-
29 [methoxy(polyethyleneoxy)propyl]-trichlorosilane (OEG-silane, Fluorochem, Hadfield, UK) in
30 toluene for 2 h. To remove the OEG-silane from the titanium dioxide the samples were exposed to a
31 325 nm UV laser (Kimmon model IK3202R-D, HeCd) at a dose of 8.65 J cm^{-2} and then rinsed with
32 ethanol and water. Protein adsorption was carried out by immersing the samples in $10 \text{ } \mu\text{L mL}^{-1}$ of
33 Streptavidin-Cy3 or IgG-FITC, pH 7.4, 10 mM phosphate buffered saline solution overnight. The
34 samples were rinsed with de-ionized water and then dried under a stream of nitrogen before
35 imaging with confocal microscopy. Subsequent removal of the protein was achieved by irradiating
36 the sample at 325 nm wavelengths with a dose of 14.4 J cm^{-2} .
37
38
39
40
41
42
43
44
45
46
47
48
49
50
51
52
53
54
55
56
57
58
59
60

IL

Interference lithography was carried out using a Lloyds mirror interferometer in conjunction with the frequency-doubled argon ion laser. The angle between the mirror and the sample in the interferometer was varied depending on the period of the pattern required. Samples were patterned using the IL with a dose of between 1.68 – 3.93 J cm⁻¹. Following photopatterning the samples were rinsed with ethanol and the titanium substrates were etched by placing in warm piranha solution (40 °C) for 4-6 min. The samples were then rinsed with de-ionized water and calcined in an oven at 550 °C for 1H.

SAMs of OEG-silane were formed on the etched samples by placing them in a 1 mM solution of OEG-silane in toluene for 2 h. To remove the OEG-silane from titania the samples were exposed to the HeCd laser at a dose of 8.65 J cm⁻² and then rinsed with ethanol and water. Protein adsorption was carried out by immersing the samples in 20 µg mL⁻¹ of GFP or YFP in pH 7.4, 100 mM ammonium acetate buffer solution overnight. The samples were rinsed with de-ionized water and then dried under a stream of nitrogen before imaging with confocal microscopy.

NIL

Titanium (IV) *n*-butoxide (97%), 2-(methacryloyloxy) ethyl acetoacetate (95%) and ethylene glycol dimethacrylate (98%) were purchased from Sigma Aldrich and used as received. Benzoyl peroxide (BPO) was supplied by Sinopharm Chemical Reagent. 2-[Methoxy(polyethyleneoxy)propyl]-trichlorosilane (OEG-silane) was supplied by Fluorochem. Absolute ethanol (99.8+%) was supplied by Fisher Scientific.

All glassware and silicon wafers used were first cleaned by submersion in piranha solution, a mixture of 30% hydrogen peroxide and 95% concentrated sulfuric acid in the ratio 3:7 for at least 40 min. (*Caution: Piranha solution is an extremely strong oxidizing agent which has been known to detonate spontaneously upon contact with organic material.*) The glassware was rinsed thoroughly

1
2
3 with deionized water (Elgar Nanopure, 18.2M Ω) a minimum of six times and then sonicated for 10
4
5 min before being placed in the oven (approximately 80 C) and left overnight to dry.
6

7
8 A titanium dioxide resin was made by combining titanium (IV) *n*-butoxide with 2-
9
10 (methacryloyloxy) ethyl acetoacetate in 1:2 molar ratio inside a glove box (<5% relative humidity)
11
12 to form the chelated precursor with an alcohol as by product. Then, ethylene glycol dimethacrylate
13
14 as a cross-linker was added to the chelated precursor followed by benzoyl peroxide (BPO), an
15
16 initiator for thermal free radical polymerization.⁴³
17

18
19 The titanium dioxide resin was spin-coated onto glass substrates at 3000 rpm for 30 s. The
20
21 monomer film was imprinted with silicon moulds using an Eitre 6 (Obducat) nanoimprinting
22
23 system. Samples were imprinted at 35 bar and for the first 300s the temperature was set at 30 °C,
24
25 then the temperature was raised to 135 °C and cured for 600 s before the pressure was released
26
27 and the mould removed. After the imprinting step, the samples were calcined in an oven at 550 °C
28
29 for 1 h. The residual layer was removed by an RIE process using a Plasmalab 80 Plus (Oxford
30
31 Instruments). The pressure and power were set at 80 mTorr and 125 W, respectively. SF₆ and Ar
32
33 gas were supplied at flow rates of 30 sccm and 10 sccm, respectively, for an etch time of 1 min. The
34
35 samples were then cleaned with fuming piranha solution and rinsed with ultra-pure DI water. SAMs
36
37 of OEG-silane were formed on the etched samples by placing them in a 1 mM solution of OEG-silane
38
39 in toluene for 2 h. The samples were then irradiated by a UV-A lamp emitting wavelengths in the
40
41 range 320 nm – 400 nm for 3 min to remove the OEG-silane molecules bound to the TiO₂ structures.
42
43 Protein adsorption was carried out by immersing the samples overnight in 10 μ L mL⁻¹ of
44
45 streptavidin-Cy5 or wheat germ agglutinin-fluorescein (WGA-FITC), pH 7.4, 10 mM phosphate
46
47 buffered saline solution. The samples were rinsed with de-ionized water and then dried under a
48
49 stream of nitrogen before imaging with confocal microscopy. Subsequent removal of the protein
50
51 was achieved analogous to the removal of the PEG-silane, by irradiating the sample with a UV-A
52
53 lamp for 3 min.
54
55
56
57
58
59
60

Preparation of GFP and YFP

The gene sequence of yellow fluorescent protein (YFP) was amplified by PCR from pCS2-Venus vector (a kind gift from Dr. Atsushi Miyawaki, RIKEN Brain science institute, Japan). The resulting Nde I /Bam HI fragment was cloned into a pET14b expression vector (Novagen). Introducing the combined F64L, S65T, V68L, S72A, M153T, V163A, S175G, A206K mutations into the YFP gene resulted in enhanced green fluorescent protein (GFP) gene⁴⁴. Both His₆-YFP and His₆-GFP proteins were produced by heterologous expression in *E. coli* (BL21); cells were grown to an O.D₆₈₀ of 0.6 at 37 °C then induced using IPTG (0.4 mM) for 12 hrs at 25 °C. Pelleted cells (19000 x g / 20 min) were lysed by sonication and the resulting lysate was clarified by a further spin (33000 x g / 30 min). Both His-tagged fluorescent proteins were purified to homogeneity from clarified lysate using a Chelating Sepharose Fast Flow Ni-NTA gravity flow column (GE Healthcare) as detailed in the manufacturer's instructions. Protein purity was assessed by gel electrophoresis (SDS-PAGE).

Characterization

XPS measurements were made using a Kratos Axis Ultra X-ray photoelectron spectrometer, equipped with a delay-line detector and operating at a base pressure of 1×10^{-9} mbar. Survey spectra were acquired at pass energy of 160 eV, and high resolution spectra at pass energy of 20 eV. All XPS spectra were analyzed and curve-fitted using the Casa XPS software, and were corrected relative to the C 1s signal at binding energy (B.E.) = 285.0 eV.

Tapping AFM measurements were made using a Bruker Nanoscope IV Multimode atomic force microscope. RTESP probes with a nominal tip radius 8 nm and TESP-SS series ultra-sharp silicon probes (Bruker), with resonance frequency of 320-350 kHz and an average tip radius of 2 nm, were used.

Fluorescence images were acquired with a LSM 510 Meta laser scanning confocal microscope (Carl Zeiss, Welwyn Garden City, UK). The samples were mounted in a glycerol/PBS- based anti fade solution (Citifluor AF1, Agar Scientific, UK) and observed with 40x and 63x oil immersion

1
2
3 objectives (numerical apertures of 1.30 and 1.40, respectively). A small drop of immersion oil
4
5 (Immersionol 518 F, Zeiss) was placed on the slide in the center of the lighted area. All fluorescence
6
7 images were analyzed using Zeiss LSM image browser software.
8

9
10 AUTHOR INFORMATION

11
12
13 *Corresponding authors. E-mail: karen-chong@imre.a-star.edu.sg, Graham.Leggett@sheffield.ac.uk.
14

15
16 ACKNOWLEDGMENT

17
18 The authors thank EPSRC (Grant EP/I012060/1) for a Programme Grant. M. M. thanks the
19
20 A*STAR-Sheffield Research Attachment Program (ARAP) for a research studentship and also the
21
22 A*STAR Nanoimprint Foundry (IMRE/13-2B0278) for project funding. CNH gratefully
23
24 acknowledges financial support from the Biotechnology and Biological Sciences Research Council
25
26 (BBSRC UK), award number BB/G021546/1. CNH was also supported by an Advanced Award
27
28 338895 from the European Research Council and as part of the Photosynthetic Antenna Research
29
30 Center (PARC), an Energy Frontier Research Center funded by the U.S. Department of Energy, Office
31
32 of Science, Office of Basic Energy Sciences under Award Number DE-SC 0001035. PARC's role was
33
34 to provide partial support for CNH.
35
36
37

38
39 REFERENCES

40
41
42 (1) Lee, S.-W.; Lee, K.-S.; Ahn, J.; Lee, J.-J.; Kim, M.-G.; Shin, Y.-B. Highly Sensitive
43
44 Biosensing Using Arrays of Plasmonic Au Nanodisks Realized by Nanoimprint Lithography. *ACS*
45
46 *Nano* **2011**, *5*, 897-904.
47

48
49 (2) Canalejas-Tejero, V.; Herranz, S.; Bellingham, A.; Moreno-Bondi, M. C.; Barrios, C. A.
50
51 Passivated Aluminum Nanohole Arrays for Label-Free Biosensing Applications. *ACS Appl. Mater.*
52
53 *Interfaces* **2013**, *6*, 1005-1010.
54
55
56
57
58
59
60

- 1
2
3 (3) Turner, A. P. F. Biosensors: Sense and Sensibility. *Chem. Soc. Rev.* **2013**, *42*, 3184-
4 3196.
5
6
7
8 (4) Ahijado-Guzmán, R.; Prasad, J.; Rosman, C.; Henkel, A.; Tome, L.; Schneider, D.; Rivas,
9 G.; Sönnichsen, C. Plasmonic Nanosensors for Simultaneous Quantification of Multiple Protein-
10 Protein Binding Affinities. *Nano Lett.* **2014**, *14*, 5528-5532.
11
12
13 (5) Lopez, G. P.; Albers, M. W.; Schreiber, S. L.; Carroll, R.; Peralta, E.; Whitesides, G. M.
14 Convenient Methods for Patterning the Adhesion of Mammalian Cells to Surfaces using Self-
15 Assembled Monolayers of Alkanethiolates on Gold. *J. Am. Chem. Soc.* **1993**, *115*, 5877-5978.
16
17
18 (6) Singhvi, R.; Kumar, A.; Lopez, G. P.; Stephanopoulos, G. N.; Wang, D. I. C.; Whitesides,
19 G. M.; Ingber, D. E. Engineering Cell Shape and Function. *Science* **1994**, *264*, 696-698.
20
21
22 (7) Chen, C. S.; Mrksich, M.; Huang, S.; Whitesides, G. M.; Ingber, D. E. Geometric control
23 of cell life and death. *Science* **1997**, *276*, 1425-1428.
24
25
26 (8) Lee, K.-B.; Park, S.-J.; Mirkin, C. A.; Smith, J. C.; Mrksich, M. Nanoarrays Generated by
27 Dip-Pen Nanolithography. *Science* **2002**, *295*, 1702-1705.
28
29
30 (9) Cavalcanti-Adam, E. A.; Volberg, T.; Micoulet, A.; Kessler, H.; Geiger, B.; Spatz, J. P.
31 Cell Spreading and Focal Adhesion Dynamics are Regulated by Spacing of Integrin Ligands. *Biophys.*
32 *J.* **2007**, *92*, 2964-2974.
33
34
35 (10) Reynolds, N. P.; Janusz, S. J.; Escalante-Marun, M.; Timney, J.; Ducker, R. E.; Olsen, J.
36 D.; Otto, C.; Subramanian, V.; Leggett, G. J.; Hunter, C. N. Directed Formation of Micro- and Nanoscale
37 Patterns of Functional Light Harvesting LH2 Complexes. *J. Am. Chem. Soc.* **2007**, *129*, 14625-14631.
38
39
40
41
42
43
44
45
46
47
48
49
50
51
52
53
54
55
56
57
58
59
60

- 1
2
3
4
5
6
7
8
9
10
11
12
13
14
15
16
17
18
19
20
21
22
23
24
25
26
27
28
29
30
31
32
33
34
35
36
37
38
39
40
41
42
43
44
45
46
47
48
49
50
51
52
53
54
55
56
57
58
59
60
- (11) Escalante, M.; Lenferink, A.; Zhao, Y.; Tas, N.; Huskens, J.; Hunter, C. N.; Subramaniam, V.; Otto, C. Long-Range Energy Propagation in Nanometer Arrays of Light Harvesting Antenna Complexes. *Nano Lett.* **2010**, *10*, 1450-1450.
- (12) Coyer, S. R.; García, A. J.; Delamarche, E. Facile Preparation of Complex Protein Architectures with Sub-100-nm Resolution on Surfaces. *Angew. Chem. Int. Ed.* **2007**, *46*, 6837-684.
- (13) Piner, R. D.; Zhu, J.; Xu, F.; Hong, S.; Mirkin, C. A. "Dip-Pen" Nanolithography. *Science* **1999**, *283*, 661-663
- (14) Lim, J.-H.; Ginger, D. S.; Lee, K.-B.; Heo, J.; Nam, J.-M.; Mirkin, C. A. Direct-Write Dip-Pen Nanolithography of Proteins on Modified Silicon Oxide surfaces. *Angew. Chem. Int. Ed.* **2003**, *42*, 2309-2312.
- (15) Zhou, D.; Wang, X.; Birch, L.; Rayment, T.; Abell, C. AFM Study on Protein Immobilization on Charged Surfaces at the Nanoscale: Toward the Fabrication of Three-Dimensional Protein Nanostructures. *Langmuir* **2003**, *19*, 10557-10562.
- (16) Ballav, N.; Thomas, H.; Winkler, T.; Terfort, A.; Zharnikov, M. Making Protein Patterns by Writing in a Protein-Repelling Matrix. *Angew. Chem. Int. Ed.* **2009**, *48*, 5833-5836.
- (17) Krakert, S.; Ballav, N.; Zharnikov, M.; Terfort, A. Adjustment of the bioresistivity by electron irradiation: self-assembled monolayers of oligo(ethyleneglycol)-terminated alkanethiols with embedded cleavable group. *Phys. Chem. Chem. Phys.* **2010**, *12*, 507-515.
- (18) Montague, M.; Ducker, R. E.; Chong, K. S. L.; Manning, R. J.; Rutten, F. J. M.; Davies, M. C.; Leggett, G. J. Fabrication of Biomolecular Nanostructures by Scanning Near-Field Photolithography of Oligo(ethylene glycol) Terminated Self-Assembled Monolayers. *Langmuir* **2007**, *23*, 7328-7337.

- 1
2
3 (19) Reynolds, N. P.; Tucker, J. D.; Davison, P. A.; Timney, J. A.; Hunter, C. N.; Leggett, G. J.
4
5 Site-Specific Immobilization and Micrometer and Nanometer Scale Photopatterning of Yellow
6
7 Fluorescent Protein on Glass Surfaces. *J. Am Chem. Soc.* **2009**, *131*, 896-897.
8
9
10 (20) Alang Ahmad, S. A.; Wong, L. S.; ul-Haq, E.; Hobbs, J. K.; Leggett, G. J.; Micklefield, J.
11
12 Protein Micro- and Nanopatterning Using Aminosilanes with Protein-Resistant Photolabile
13
14 Protecting Groups. *J. Am. Chem. Soc.* **2011**, *133*, 2749-2759.
15
16
17 (21) Alswieleh, A. M.; Cheng, N.; Canton, I.; Ustbas, B.; Xue, X.; Ladmiral, V.; Xia, S.; Ducker,
18
19 R. E.; El Zubir, O.; Cartron, M. L.; *et al.* Zwitterionic Poly(amino acid methacrylate) Brushes. *J. Am.*
20
21 *Chem. Soc.* **2014**, *136*, 9404-9413.
22
23
24 (22) Tizazu, G.; el Zubir, O.; Patole, S.; McLaren, A.; Vasilev, C.; Mothersole, D.; Adawi, A.;
25
26 Hunter, C. N.; Lidzey, D.; Lopez, G.; *et al.* Micrometer and Nanometer Scale Photopatterning of
27
28 Proteins on Glass Surfaces by Photo-degradation of Films Formed from Oligo(Ethylene Glycol)
29
30 Terminated Silanes. *Biointerphases* **2012**, *7*, 1-9.
31
32
33 (23) Wang, R.; Hashimoto, K.; Fujishima, A.; Chikuni, M.; Kojima, E.; Kitamura, A.;
34
35 Shimohigoshi, M.; Watanabe, T. Light-Induced Amphiphilic Surfaces. *Nature* **1997**, *388*, 431-432.
36
37
38 (24) Haick, H.; Paz, Y. Remote Photocatalytic Activity as Probed by Measuring the
39
40 Degradation of Self-Assembled Monolayers Anchored near Microdomains of Titanium Dioxide. *J.*
41
42 *Phys. Chem. B* **2001**, *105*, 3045-3054.
43
44
45 (25) Haick, H.; Paz, Y. "Dark" Photocatalysis: The Degradation of Organic Molecules
46
47 Anchored to Dark Microdomains of Titanium Dioxide. *Chem. Phys. Chem.* **2003**, *4*, 617-620.
48
49
50
51
52
53
54
55
56
57
58
59
60

- 1
2
3
4 (26) Lee, J. P.; Kim, H. K.; Park, C. R.; Park, G.; Kwak, H. T.; Koo, S. M.; Sung, M. M.
5
6 Photocatalytic Decomposition of Alkylsiloxane Self-Assembled Monolayers on Titanium Oxide
7
8 Surfaces. *J. Phys. Chem. B* **2003**, *107*, 8997-9002.
9
10
11 (27) Blondiaux, N.; Zurcher, S.; Liley, M.; Spencer, N. D. Fabrication of Multiscale Surface-
12
13 Chemical Gradients by Means of Photocatalytic Lithography. *Langmuir* **2007**, *23*, 3489-3494.
14
15
16 (28) Soja, G. R.; Watson, D. F. TiO₂-Catalyzed Photodegradation of Porphyrins:
17
18 Mechanistic Studies and Application in Monolayer Photolithography. *Langmuir* **2009**, *25*, 5398-
19
20 5403.
21
22
23 (29) Tizazu, G.; Adawi, A.; Leggett, G. J.; Lidzey, D. G. Photopatterning, Etching, and
24
25 Derivatization of Self-Assembled Monolayers of Phosphonic Acids on the Native Oxide of Titanium.
26
27 *Langmuir* **2009**, *25*, 10746-10753.
28
29
30
31 (30) Nakata, K.; Nishimoto, S.; Yuda, Y.; Ochiai, T.; Murakami, T.; Fujishima, A. Rewritable
32
33 Superhydrophilic-Superhydrophobic Patterns on a Sintered Titanium Dioxide Substrate. *Langmuir*
34
35 **2010**, *26*, 11628-11630.
36
37
38 (31) Paz, Y. Self-assembled monolayers and titanium dioxide: From surface patterning to
39
40 potential applications. *Beilstein J. Nanotechnol.* **2011**, *2*, 845-861.
41
42
43 (32) Zhang, L.; Diao, S.; Nie, Y.; Yan, K.; Liu, N.; Dai, B.; Xie, Q.; Reina, A.; Kong, J.; Liu, Z.
44
45 Photocatalytic Patterning and Modification of Graphene. *J. Am. Chem. Soc.* **2011**, *133*, 2706-2713.
46
47
48 (33) Kobayashi, K.; Tomita, Y.; Maeda, Y. Nanolithography Based on Photocatalysis of TiO
49
50 2 Using an Atomic Force Microscope. *Japan. J. Appl. Physics* **2005**, *44*, 5829-583.
51
52
53
54
55
56
57
58
59
60

- 1
2
3 (34) Ul-Haq, E.; Patole, S.; Moxey, M.; Amstad, E.; Vasilev, C.; Hunter, C. N.; Leggett, G. J.;
4
5 Spencer, N. D.; Williams, N. H. Photocatalytic Nanolithography of Self-Assembled Monolayers and
6
7 Proteins. *ACS Nano* **2013**, *7*, 7610-761810.
8
9
10 (35) Brueck, S. R. J. Optical and Interferometric Lithography - Nanotechnology Enablers.
11
12 *Proc. IEEE* **2005**, *93*, 1704-172.
13
14
15 (36) Textor, M.; Ruiz, L.; Hofer, R.; Rossi, A.; Feldman, K.; Hahner, G.; Spencer, N. D.
16
17 Structural Chemistry of Self-Assembled Monolayers of Octadecylphosphonic Acid on Tantalum
18
19 Oxide Surfaces *Langmuir* **2000**, *16*, 3257-3271.
20
21
22 (37) Tosatti, S.; Michel, R.; Textor, M.; Spencer, N. D. Self-Assembled Monolayers of
23
24 Dodecyl and Hydroxy-dodecyl Phosphates on Both Smooth and Rough Titanium and Titanium
25
26 Oxide Surfaces. *Langmuir* **2002**, *18*, 3537-3548.
27
28
29 (38) Zwahlen, M.; Tosatti, S.; Textor, M.; Hahner, G. Orientation in Methyl- and Hydroxyl-
30
31 Terminated Self-Assembled Alkanephosphate Monolayers on Titanium Oxide Surfaces Investigated
32
33 with Soft X-Ray Absorption. *Langmuir* **2002**, *18*, 3957-3962.
34
35
36 (39) Spori, D. M.; Venkataraman, N. V.; Tosatti, S. G. P.; Durmaz, F.; Spencer, N. D.; Zurcher,
37
38 S. Influence of Alkyl Chain Length on Phosphate Self-Assembled Monolayers. *Langmuir* **2007**, *23*,
39
40 8053-8060.
41
42
43 (40) Ramsier, R. D.; Henriksen, P. N.; A.N., G. Adsorption of Phosphorus Acids on Alumina.
44
45 *Surf. Sci.* **1988**, *203*, 72-88.
46
47
48 (41) Gao, W.; Dickinson, L.; Grozinger, C.; Morin, F. G.; Reven, L. Self-Assembled
49
50 Monolayers of Alkylphosphonic Acids on Metal Oxides. *Langmuir* **1996**, *12*, 6429-6435.
51
52
53
54
55
56
57
58
59
60

1
2
3 (42) Cao, G.; Hong, H.-G.; Mallouk, T. E. Layered Metal Phosphates and Phosphonates:
4 From Crystals to Monolayers. *Acc. Chem. Res.* **1992**, *25*, 420-427.
5
6

7
8 (43) Dinachali, S. S.; Saifullah, M. S. M.; Ganesan, R.; Thian, E. S.; He, C. A Universal Scheme
9 for Patterning of Oxides *via* Thermal Nanoimprint Lithography. *Adv. Funct. Mater.* **2013**, *23*, 2201-
10 2211.
11
12
13

14
15 (44) Kramers, G. J.; Goedhart, J.; van Munster, E. B.; Gadella, T. W. J. Cyan and Yellow
16 Super Fluorescent Proteins with Improved Brightness, Protein Folding, and FRET Förster Radius.
17
18
19
20
21
22
23
24
25
26
27
28
29
30
31
32
33
34
35
36
37
38
39
40
41
42
43
44
45
46
47
48
49
50
51
52
53
54
55
56
57
58
59
60
Biochemistry **2006**, *45*, 6570-6580.

1
2
3
4
5
6
7
8
9
10
11
12
13
14
15
16
17
18
19
20
21
22
23
24
25
26
27
28
29
30
31
32
33
34
35
36
37
38
39
40
41
42
43
44
45
46
47
48
49
50
51
52
53
54
55
56
57
58
59
60

TOC Graphic

